Eikonal calculation of $(p, 3p)$ cross sections for neutron-rich nuclei

M. Gómez-Ramos *

Departamento de FAMN, Universidad de Sevilla, Apartado 1065, 41080 Sevilla, Spain
and Institut für Kernphysik, Technische Universität Darmstadt, D-64289 Darmstadt, Germany

(Received 24 April 2024; accepted 3 June 2024; published 24 June 2024)

In this work, I present the first, to my knowledge, theoretical description of two-proton removal reactions with proton target $(p, 3p)$ for medium-mass nuclei at intermediate energies and present cross sections for the different bound states of the residual nucleus with two fewer protons. The description of the reaction assumes two sequential "quasifree" collisions between the target and removed protons and considers eikonal propagation in between. The formalism is applied to the reactions ^{12}C$(p, 3p)$ ^{10}Be, ^{28}Mg$(p, 3p)$ ^{26}Ne, and ^{54}Ca$(p, 3p)$ ^{52}Ar, finding reasonable agreement to experimental data for the ^{12}C target and an overestimation of a factor $\approx$3 for the more neutron-rich and ^{54}Ca, which is similar to the results found in two-proton knockout experiments with ^{9}Be and ^{12}C targets.

DOI: 10.1103/PhysRevC.109.064622

I. INTRODUCTION

Two-proton knockout reactions from neutron-rich nuclei using ^{9}Be and ^{12}C at intermediate energies have been shown to proceed as a direct reaction [1] and were shown to be able to populate very exotic nuclei via the removal of two protons from already proton-deficient nuclei [1,2]. Equivalently, two-neutron knockout reactions from proton-rich nuclei have been used to study very neutron-rich nuclei [3]. The analysis of these reactions using an eikonal sudden description [4,5] has yielded significant results on the structure of these nuclei [6–10] and on the effect of nuclear correlations on the observables of the reactions, and therefore their value as a probe of these correlations [3,5,11–13]. The development of new hydrogen-target detectors, such as active targets [14], or MINOS [15], where a thick liquid-hydrogen target is coupled to a vertex tracker for the recoil protons, has opened the use of proton-induced reactions as reliable probes to explore exotic nuclei, where the reaction mechanism can be explored and understood thanks to the tracking of the paths of the outgoing particles. Therefore, two-proton removal reactions with proton targets, or $(p, 3p)$, appear as an appealing probe to produce exotic nuclei by removing two protons from already proton-deficient species, and to be able to study their properties thanks to the simpler reaction mechanism and the possibility for proton tracking. Unfortunately, as was the case for one-neutron removal, the reaction models used with heavier targets [16] are not applicable for the case of the proton target, due to the significant recoil of the target proton. Models considering a "quasifree" interaction between removed and target protons have been more successful in the description of the experimental data for reactions with proton targets $(p, 2p)$ [17–20], so a similar approach for $(p, 3p)$ reactions seems promising and is required in order to fully exploit $(p, 3p)$ reactions as a spectroscopic tool using the experimental possibility that hydrogen active targets provide. This need has been indicated in previous publications [21] where the lack of such a theory has hindered the analysis of the experimental data.

This work aims to provide a theoretical formalism for $(p, 3p)$ reactions, based on the assumption of "quasifree" collision between the target and removed protons, and is structured as follows. Section II presents the theoretical formalism and briefly shows its derivation, Sec. III presents calculations of $(p, 3p)$ reactions for the stable ^{12}C target as validation of the theory and results for the neutron-rich targets ^{28}Mg and ^{54}Ca. Finally, Sec. IV presents the conclusions and summary of this work as well as future extensions.

II. THEORETICAL FRAMEWORK

A process $p + (A + 2) \rightarrow 3p + A$ is considered, where a projectile proton collides with the target nucleus $A + 2$ removing two protons from it, with the remaining nucleus A remaining bound. For the derivation, an infinite mass for A will be assumed. Following the results from [22], the process is described as two sequential and independent collisions between the projectile proton and two protons of the target, with the residual nucleus A remaining as an inert spectator. It will also be assumed that the reaction occurs fast enough for the internal degrees of freedom of A to remain frozen during the collision, so that the removal of the two protons does not alter the state of A. For ease of description, in this derivation, the protons will be treated as distinguishable, since, following Goldberger and Watson [23], it is sufficient to consider their antisymmetrization in the proton-proton interaction V_{pp}. As such, p_0 corresponds to the incoming proton, with momentum $\hbar\mathbf{k}_0$. p_0 is then assumed to collide with the first proton p_1, which is expelled with an asymptotic momentum $\hbar\mathbf{k}_1$. Then p_0 collides with a second proton p_2, and both escape the

*Contact author: mgomez40@us.es

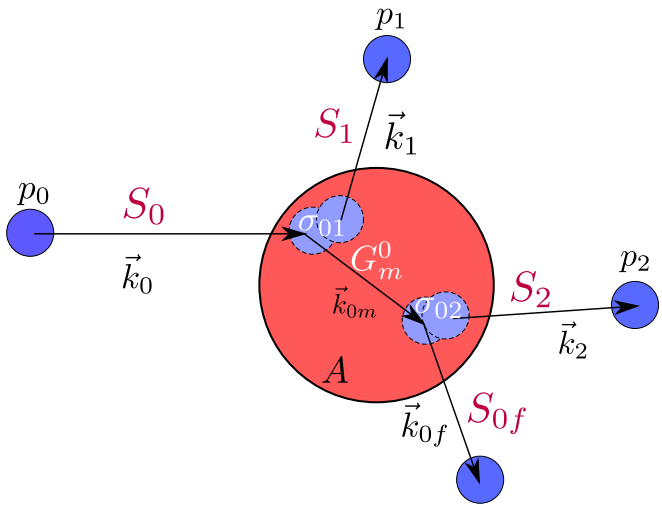

FIG. 1. Schematic description of the reaction model considered in this work, two sequential collisions of the incoming proton with the removed protons. The labels used in this work are presented in black, indicating as well the wave numbers of the protons at each step of the process. The elements appearing in the T matrix for the reaction can be associated to the different steps of the trajectory of the protons and are shown close to them in purple and white.

nucleus with momenta $\hbar\mathbf{k}_{0f}$ and $\hbar\mathbf{k}_2$, respectively. Through momentum conservation the residual nucleus A is left with momentum $\hbar\mathbf{k}_A = \hbar(\mathbf{k}_0 - \mathbf{k}_{0f} - \mathbf{k}_1 - \mathbf{k}_2)$. A diagram of the process is shown in Fig. 1. Schematically, the transition matrix for this process can be expressed as

$$T \approx \int \mathrm{d}\xi \prod_i (\mathrm{d}\mathbf{r}_i)\chi^*_{p_0}(\mathbf{r}_{0f}, \mathbf{k}_{0f})\chi^*_{p_1}(\mathbf{r}_1, \mathbf{k}_1)\chi^*_{p_2}(\mathbf{r}_2, \mathbf{k}_2) \times \Phi_A(\xi_A)[V_{02}GV_{01}](\mathbf{r}_{0f}, \mathbf{r}_1, \mathbf{r}_2, \xi_A; \mathbf{r}_0, \xi)\Phi_{(A+2)}(\xi)\chi_{p_0} \times (\mathbf{r}_0, \mathbf{k}_0), \quad (1)$$

where $\mathrm{d}\mathbf{r}_i$ denotes all radial variables involved: $\mathbf{r}_{0f}$, $\mathbf{r}_1$, $\mathbf{r}_2$, $\mathbf{r}_0$; χ_{p_i} indicate the wave functions for the relative motion between the corresponding particles and residual nucleus A (with infinite mass) for the corresponding asymptotic momenta, ξ and ξ_A correspond to the internal coordinates of $(A+2)$ and A, respectively, V_{ij} is the interaction potential between protons i and j and G is the propagator of the system. Due to the spectator approximation for A its internal coordinates ξ_A are not modified during the reaction, so neither V nor G depend on them. The expansion $\xi_{(A+2)} = \xi_A, \mathbf{r}_{1i}, \mathbf{r}_{2i}$ can be performed, where $\mathbf{r}_{ji}$ is the position of proton j "within" $(A+2)$. Thus, the overlap between $(A+2)$ and A can be computed as

$$\int \mathrm{d}\xi_A \langle A(\xi_A)|(A+2)(\xi_A, \mathbf{r}_{1i}, \mathbf{r}_{2i})\rangle = \phi_{12}(\mathbf{r}_{1i}, \mathbf{r}_{2i}). \quad (2)$$

It should be noted that $\phi_{12}(\mathbf{r}_{1i}, \mathbf{r}_{2i})$ is independent of the reaction and can be obtained via structure calculations such as nuclear shell model [4]. This results in the T matrix

$$T \approx \int \mathrm{d}\mathbf{r}_{0f}\mathrm{d}\mathbf{r}_1\mathrm{d}\mathbf{r}_2\mathrm{d}\mathbf{r}_0\mathrm{d}\mathbf{r}_{1i}\mathrm{d}\mathbf{r}_{2i}\chi^*_{p_0}(\mathbf{r}_{0f}, \mathbf{k}_{0f})\chi^*_{p_1}(\mathbf{r}_1, \mathbf{k}_1)\chi^*_{p_2}(\mathbf{r}_2, \mathbf{k}_2)[V_{02}GV_{01}](\mathbf{r}_{0f}, \mathbf{r}_1, \mathbf{r}_2; \mathbf{r}_0, \mathbf{r}_{1i}, \mathbf{r}_2)\chi_{p_0}(\mathbf{r}_0, \mathbf{k}_0)\phi_{12}(\mathbf{r}_{1i}, \mathbf{r}_{2i}). \quad (3)$$

The propagator G can be approximated as [24]

$$G = G_{01} + GV_{01}G_{01} \approx G_{01}, \quad (4)$$

which corresponds to

$$G_{01} = \frac{1}{E - H - V_{01} + i\epsilon} = \frac{1}{E - T_1 - T_2 - T_0 - V_{02} - U_{0A} - U_{1A} - V_{2A} - V_{12} + i\epsilon}, \quad (5)$$

where the infinite mass approximation for A allows to remove its kinetic energy. This four-body propagator must now be reduced to a one-body one. For this, (since $A \to \infty$) T_2 and V_{2A} can be grouped as $T_2 + V_{2A} \approx H_{2A}$, and the propagator approximated as

$$H_{2A}\phi_{12}(\mathbf{r}_{1i}, \mathbf{r}_{2i}) \approx E_{2A}\phi_{12}(\mathbf{r}_{1i}, \mathbf{r}_{2i}) \approx \frac{S_{2p}}{2}\phi_{12}(\mathbf{r}_{1i}, \mathbf{r}_{2i}). \quad (6)$$

This assumption should be reasonable for an energetic beam, as p_2 should remain frozen before its collision and $E_{2A} \ll E$. Analogously $T_1 + U_{1A} + V_{12} = H_{1(A+1)}$, which can be approximated as

$$\chi^*_{p_1}(\mathbf{r}_1, \mathbf{k}_1)H_{1(A+1)} = \chi^*_{p_1}(\mathbf{r}_1, \mathbf{k}_1)E_1, \quad (7)$$

and finally $U_{0A} + V_{02} \approx U_{0(A+1)}$. With these approximations, the propagator reduces to

$$G_{01} = \frac{1}{E - E_1 - E_{2A} - T_0 - U_{0(A+1)} + i\epsilon} = \frac{1}{E_{0m} - T_0 - U_{0(A+1)} + i\epsilon}, \quad (8)$$

where $E_{0m} = E - E_1 - E_{2A}$ and which can be interpreted as a one-body propagator for p_0 between collisions. The beam energy will be assumed high so that E_1 is large enough for the effect of the potential to be ignored, so that $E_1 = \sqrt{m_p^2 + \hbar^2 k_1^2}$ $(c = 1)$.

The proton-proton interaction is then considered to be of zero range so that

$$V_{01}(\mathbf{r}'_0, \mathbf{r}'_1; \mathbf{r}_0, \mathbf{r}_1) = \tilde{V}_{01}\delta(\mathbf{r}'_0, \mathbf{r}'_1, \mathbf{r}_0, \mathbf{r}_1). \quad (9)$$

With these approximations, the integral in Eq. (3) is reduced to only two radial coordinates $\mathbf{r}_1, \mathbf{r}_2$, which can be interpreted as the location of the collisions between p_0 and p_1 and between p_0 and p_2, respectively:

$$T \approx \int \mathrm{d}\mathbf{r}_1 \mathrm{d}\mathbf{r}_2 \chi^*_{p_0}(\mathbf{r}_2, \mathbf{k}_{0f}) \chi^*_{p_1}(\mathbf{r}_1, \mathbf{k}_1) \chi^*_{p_2}(\mathbf{r}_2, \mathbf{k}_2) \times \tilde{V}_{02} G_{0m}(E_{0m}, \mathbf{r}_2; \mathbf{r}_1) \tilde{V}_{01} \chi_{p_0}(\mathbf{r}_1, \mathbf{k}_0) \phi_{12}(\mathbf{r}_1, \mathbf{r}_2). \quad (10)$$

Eikonal expressions for the wave functions are now introduced:

$$\chi_{p_n}(\mathbf{r}_j, \mathbf{k}_i) = \frac{1}{(2\pi)^{3/2}} e^{-\frac{i}{\hbar v_i}\int_{-\infty}^{z_j} U(\mathbf{b}_j, z)\mathrm{d}z} e^{i\mathbf{k}_0\mathbf{r}_1} = \frac{1}{(2\pi)^{3/2}} S_{p0}(\mathbf{r}_1, \mathbf{k}_0) e^{i\mathbf{k}_0\mathbf{r}_1}, \quad (11)$$

where z follows the direction of momentum $\mathbf{k}_i$, $\mathbf{b}$ is the associated impact parameter and U is the optical potential between proton and core A (As $A \to \infty$, $U_{pA} \approx U_{p(A+1)} \approx U_{p(A+2)}$). With this approximation the following matrix element is obtained:

$$T = \frac{1}{(2\pi)^6} \int \mathrm{d}\mathbf{k}_{0m} \mathrm{d}\mathbf{r}_1 \mathrm{d}\mathbf{r}_2 S^*(\mathbf{r}_2, \mathbf{k}_{0f}) S^*(\mathbf{r}_2, \mathbf{k}_2) \times \tilde{V}_{02} G_{0m}(E_{0m}, \mathbf{r}_2; \mathbf{r}_1) \tilde{V}_{01} S^*(\mathbf{r}_1, \mathbf{k}_1) S(\mathbf{r}_1, \mathbf{k}_0) \phi_{12}(\mathbf{r}_1, \mathbf{r}_2) \times e^{i(\mathbf{k}_0 - \mathbf{k}_1)\mathbf{r}_1} e^{-i(\mathbf{k}_{0f} + \mathbf{k}_2)\mathbf{r}_2}. \quad (12)$$

Next the formula for the total cross section is presented, where momentum conservation has already been considered to nullify the integral over $\mathbf{k_A}$:

$$\sigma = \frac{1}{2\hat{J}_i^2} \sum_{S, s_0, s_{0f}} \int \mathrm{d}\mathbf{k}_1 \mathrm{d}\mathbf{k}_{0f} \mathrm{d}\mathbf{k}_2 \delta(E_f - E_i) \frac{(2\pi)^4}{\hbar v_0} |T|^2, \quad (13)$$

where J_i is the angular momentum of $(A+2)$ $\hat{J}_i = \sqrt{2J_i + 1}$, the sum over S corresponds to the sum over the spin projections of $(A+2), A, p_1, p_2$ and the sums for the final and initial spin of proton p_0 are left explicit. $\mathrm{d}\mathbf{k_{0f}}$ will be now expressed in spherical coordinates and the integral over k_{0f} will be performed using $\delta(E_f - E_i)$. Thus the following result is obtained:

$$\int \mathrm{d}k_{0f} \delta(E_f - E_i) \mathcal{F}(k_{0f}) = \mathcal{F}(\bar{k}_{0f}) \left.\frac{1}{\frac{\partial E_f}{\partial k_{0f}}}\right|_{\bar{k}_{0f}} = \frac{1}{\frac{\hbar^2 c^2 \bar{k}_{0f}}{\bar{\epsilon}_{0f}} + \frac{\hbar^2 c^2 \bar{k}_{0f}}{\bar{\epsilon}_2} - \frac{\hbar^2 c^2 \bar{\mathbf{k}}_{0f}(\mathbf{k}_0 - \mathbf{k}_1 - \mathbf{k}_A)}{k_{0f}\bar{\epsilon}_2}} \mathcal{F}(\bar{k}_{0f}) \equiv j(\hat{\mathbf{k}}_{0f}, \mathbf{k}_1, \mathbf{k}_A) \mathcal{F}(\bar{k}_{0f}), \quad (14)$$

where $j(\hat{\mathbf{k}}_{0f}, \mathbf{k}_1, \mathbf{k}_A)$ corresponds to these kinematic factors and $\mathcal{F}(k_{0f})$ is meant to denote the rest of integral in Eq. (13) and where it has been applied that $k_2^2 = k_{0f}^2 - 2\mathbf{k}_{0f}(\mathbf{k}_0 - \mathbf{k}_1 - \mathbf{k}_A) + |\mathbf{k}_0 - \mathbf{k}_1 - \mathbf{k}_A|^2$ and where $\bar{\mathbf{k}}_{0f}, \bar{\epsilon}_{0f}, \bar{\epsilon}_2$ correspond to the momentum for p_{0f} and energies of p_{0f} and p_2 given by energy conservation.

To proceed with the derivation, a strong approximation is now introduced: all factors in Eqs. (12) and (13) are considered as slowly varying functions of the momentum compared to the exponentials in Eq. (12) and can be replaced by a suitable average value which may depend on $\mathbf{r_1}, \mathbf{r_2}$:

$$S(\mathbf{r}_i, \mathbf{k}_j) \approx S(\hat{\mathbf{k}}_{0f}, \mathbf{r}_1, \mathbf{r}_2), \quad j(\hat{\mathbf{k}}_{0f}, \mathbf{k}_1, \mathbf{k}_A) \approx j(\hat{\mathbf{k}}_{0f}, \mathbf{r}_1, \mathbf{r}_2), \quad (15)$$

which is a general expression, although some of the S matrices may not depend on all variables. With this approximation, Eq. (12) can be expressed as

$$T \approx \frac{1}{(2\pi)^6} \int \mathrm{d}\mathbf{r}_1 \mathrm{d}\mathbf{r}_2 \tilde{S_{0f}}^*(\hat{\mathbf{k}}_{0f}, \mathbf{r}_2, \mathbf{r}_1) \tilde{S_2}^*(\hat{\mathbf{k}}_{0f}, \mathbf{r}_2, \mathbf{r}_1) \times \tilde{G}_{0m}(E_{0m}, \mathbf{r}_2; \mathbf{r}_1) \tilde{S_1}^*(\mathbf{r}_1, \mathbf{r}_2) \tilde{S_0}(\mathbf{r}_1) |\phi_{12}|^2(\mathbf{r}_1, \mathbf{r}_2) \times \tilde{V_{01}}(\mathbf{r}_1; \mathbf{r}_2) \tilde{V_{02}}(\mathbf{r}_1; \mathbf{r}_2) e^{i(\mathbf{k}_0 - \mathbf{k}_1)\mathbf{r}_1} e^{-i(\mathbf{k}_{0f} + \mathbf{k}_2)\mathbf{r}_2}, \quad (16)$$

and now the integrals over $\mathbf{k}_1$ and $\mathbf{k}_A$ can be performed, noting that T and T^* would produce equivalent and complex conjugate exponentials with spatial variables $(\mathbf{r}_1, \mathbf{r}_2)$ and $(\mathbf{r}'_1, \mathbf{r}'_2)$:

$$\int \mathrm{d}\mathbf{k}_1 \mathrm{d}\mathbf{k}_2 \left[e^{-i\mathbf{k}_1(\mathbf{r}_1 - \mathbf{r}'_1)} e^{i\mathbf{k}_2(\mathbf{r}_2 - \mathbf{r}'_2)}\right] = (2\pi)^6 \delta(\mathbf{r}_2 - \mathbf{r}'_2) \delta(\mathbf{r}_1 - \mathbf{r}'_1), \quad (17)$$

which produces the nice result that the integral reduces to an incoherent sum over the two collision points $\mathbf{r}_1$ and $\mathbf{r}_2$, which is consistent with the semiclassical assumption

$$\sigma = \frac{1}{2\hat{J}_i^2} \sum_{S, s_0, s_{0f}} \int \mathrm{d}\hat{\mathbf{k}}_{0f} \mathrm{d}\mathbf{r}_1 \mathrm{d}\mathbf{r}_2 \times \frac{1}{\hbar v_0 (2\pi)^2} j(\hat{\mathbf{k}}_{0f}, \mathbf{r}_1, \mathbf{r}_2) |\tilde{S_{0f}}|^2(\hat{\mathbf{k}}_{0f}, \mathbf{r}_2, \mathbf{r}_1) |\tilde{S_2}|^2 \times (\hat{\mathbf{k}}_{0f}, \mathbf{r}_2, \mathbf{r}_1) \tilde{V_{02}}(\mathbf{r}_1; \mathbf{r}_2)|^2 |\tilde{G}_{0m}|^2(E_{0m}, \mathbf{r}_2; \mathbf{r}_1) \times |\tilde{S_1}|^2(\mathbf{r}_1, \mathbf{r}_2) |\tilde{V_{01}}(\mathbf{r}_1; \mathbf{r}_2)|^2 |\tilde{S_0}(\mathbf{r}_1)|^2 |\phi_{12}|^2(\mathbf{r}_1, \mathbf{r}_2). \quad (18)$$

Using now the eikonal expression for the propagator [23,25],

$$G_{0m}(E_{0m}, \mathbf{r}_2; \mathbf{r}_1) = -\frac{\epsilon_{0m}}{2\pi\hbar^2 c^2} \frac{e^{-\frac{i}{\hbar v_{0m}}\int_{z_1}^{z_2} U(\mathbf{b}, z)\mathrm{d}z}}{|\mathbf{r_2} - \mathbf{r_1}|} e^{-ik_{0m}|\mathbf{r_2} - \mathbf{r_1}|}, \quad (19)$$

where the energy E_{0m} is assumed large enough so that the integral can be performed along the straight line between r_2 and r_1 and where $\hbar k_{0m}$ is the momentum associated to E_{0m}.

A similar method for calculating the $(p, 2p)$ total cross section was presented in [18]. The average values to be used must now be chosen for each quantity. For the S matrices and propagator G_{0m} Eqs. (11) and (19) provide eikonal expressions. For $|\tilde{V_{01}}(\mathbf{r}_1; \mathbf{r}_2)|^2$ on-shell quasifree collisions between the protons will be considered, assuming the removed protons to be initially at rest, although their binding energy, taken as $S_{2p}/2$, will be taken into account. Therefore in the first collision, proton p_0 collides with momentum $\hbar\mathbf{k}_0$ with proton p_1 and both are emitted with momenta $\hbar\mathbf{k}_{0m}$ and $\hbar\mathbf{k}_1$, respectively. The direction of $\mathbf{k}_{0m}$ is parallel to $(\mathbf{r}_2 - \mathbf{r}_1)$, which is consistent with eikonal propagation. As such, positions $\mathbf{r}_1$ and $\mathbf{r}_2$ along with energy and momentum conservation in the quasifree collision define k_{0m} and $\mathbf{k}_1$. For the second collision,

assuming the proton impacts with momentum $\hbar\mathbf{k}_{0m}$, the direction of $\mathbf{k}_{0f}$ restricts the value of $\mathbf{k_2}$ and the modulus of k_{0f}, to be used in S_2 and S_{0f}, taking $\mathbf{k}_A$ as 0. Finally, $|\tilde{V_{01}}(\mathbf{r}_1;\mathbf{r}_2)|^2$ can be obtained from the free $p-p$ cross section (omitting Coulomb interaction) assuming the Born approximation

$$|\tilde{V_{01}}(\mathbf{r_1};\mathbf{r_2})|^2 \approxeq |\tilde{T_{01}}(\mathbf{r_1};\mathbf{r_2})|^2. \tag{20}$$

Moving to the NN center of mass system, introducing the adequate Möller factor the p-p T matrix becomes

$$|\tilde{T_{01}}(\mathbf{r}_1;\mathbf{r}_2)|^2 = |\tilde{T_{01}}(\mathbf{r}_1;\mathbf{r}_2)|^2_{NN}\frac{\epsilon_{cmi,0}\epsilon_{cmi,1}\epsilon^2_{cmf,1}}{(m_Nc^2 - S_{2p}/2)\epsilon_0\epsilon_1\epsilon_{0m}}, \tag{21}$$

where, since the collision happens between a proton and a pseudoproton of mass $(m_Nc^2 - S_{2p}/2)$, the center of mass energies of both particles are not the same before the collision ($\epsilon_{cmi,0}$ being the one of the proton and $\epsilon_{cmi,1}$ the one of the pseudoproton) but they are the same after the collision ϵ_{cmf}, since both outgoing particles are protons. The relation between ϵ_{cmi} and ϵ_{cmf} can be obtained through the Mandelstan variable s. The NN center of mass T matrix can be related to the angular differential free NN cross section [20], which will be approximate by the total cross section divided by 4π:

$$|\tilde{T_{01}}(\mathbf{r}_1;\mathbf{r}_2)|^2_{NN} = \frac{4(2\pi)^2\hbar^4c^4}{\epsilon^2_{cmf,1}}\frac{\mathrm{d}\sigma}{\mathrm{d}\Omega} = 2\frac{4(2\pi)^2\hbar^4c^4}{\epsilon^2_{cmf,1}}\frac{\sigma_{NN}}{4\pi} \tag{22}$$

(factor 2 due to antisymmetrization), getting

$$\begin{aligned}|\tilde{V_{01}}(\mathbf{r}_1;\mathbf{r}_2)|^2 &\approxeq 4(2\pi)\hbar^4c^4\sigma_{NN}(\mathbf{r}_1;\mathbf{r}_2)\\ &\times \frac{\epsilon_{cmi,0}\epsilon_{cmi,1}}{(m_Nc^2 - S_{2p}/2)\epsilon_0\epsilon_1\epsilon_{0m}}\\ &\equiv \sigma_{NN}(\mathbf{r}_1;\mathbf{r}_2)f(\mathbf{r}_1,\mathbf{r}_2),\end{aligned} \tag{23}$$

where the factors multiplying the nucleon-nucleon cross section σ_{NN} are included in $f(\mathbf{r}_1,\mathbf{r}_2)$. This approximation for the nucleon-nucleon interaction makes it spin-independent. Therefore the projection of the spin of p_0 must be the same in the incoming and outgoing channels, so that $\sum_{s_0,s_{0f}} = 2$, which cancels with the factor $1/2$ in Eq. (13). This results in the following expression for the cross section:

$$\begin{aligned}\sigma = &\frac{1}{\hat{J}_i^2}\sum_S\int \mathrm{d}\hat{\mathbf{k}}_{0f}\mathrm{d}\mathbf{r}_1\mathrm{d}\mathbf{r}_2\\ &\times\frac{1}{\hbar v_0(2\pi)^2}j(\hat{\mathbf{k}}_{0f},\mathbf{r}_1,\mathbf{r}_2)f_{02}(\hat{\mathbf{k}}_{0f},\mathbf{r}_1,\mathbf{r}_2)f_{01}(\mathbf{r}_1,\mathbf{r}_2)\\ &\times|\tilde{S_{0f}}|^2(\hat{\mathbf{k}}_{0f},\mathbf{r}_2,\mathbf{r}_1)|\tilde{S_2}|^2(\hat{\mathbf{k}}_{0f},\mathbf{r}_2,\mathbf{r}_1)\sigma_{02}(\mathbf{r}_1;\mathbf{r}_2)\tilde{G}_0^m\\ &\times(\mathbf{r}_2,\mathbf{r}_1)|^2|\tilde{S_1}|^2(\mathbf{r}_1,\mathbf{r}_2)\sigma_{01}(\mathbf{r}_1;\mathbf{r}_2)|\tilde{S_0}(\mathbf{r}_1)|^2|\phi_{12}|^2(\mathbf{r}_1,\mathbf{r}_2),\end{aligned} \tag{24}$$

which allows for a very classical interpretation: proton p_0 penetrates inside the nucleus with probability $|\tilde{S}_0|^2$ until it collides with cross section σ_{01} with one of the protons p_1 in the nucleus at $\mathbf{r}_1$ and then propagates to $\mathbf{r}_2$ through $|\tilde{G}_{0m}|^2$ where it collides with the second proton p_2 with cross section σ_{02}, with the probability of finding both protons at these positions given by $|\phi_{12}|^2$ for a certain state of the residual core. Afterwards, all three protons must escape the nucleus with probabilities $|\tilde{S}_{0f}|^2$, $|\tilde{S}_1|^2$, and $|\tilde{S}_2|^2$, for them to be detected. See Fig. 1 for a schematic with the factors associated to the paths of the protons. For a more compact expression, which is also more comparable with the ones in the literature, the spin average and sum will be included in $|\phi_{12}|^2$, noting that it is the only term which is sensitive to the spins of the protons

$$|\tilde{\phi}_{12}|^2(\mathbf{r}_1,\mathbf{r}_2) = \frac{1}{\hat{J}_i^2}\sum_S|\phi_{12}|^2(\mathbf{r}_1,\mathbf{r}_2) \tag{25}$$

resulting in

$$\begin{aligned}\sigma = &\int \mathrm{d}\hat{\mathbf{k}}_{0f}\mathrm{d}\mathbf{r}_1\mathrm{d}\mathbf{r}_2\frac{1}{\hbar v_0(2\pi)^2}j(\hat{\mathbf{k}}_{0f},\mathbf{r}_1,\mathbf{r}_2)f_{02}(\hat{\mathbf{k}}_{0f},\mathbf{r}_1,\mathbf{r}_2)\\ &\times f_{01}(\mathbf{r}_1,\mathbf{r}_2)|\tilde{S_{0f}}|^2(\hat{\mathbf{k}}_{0f},\mathbf{r}_2,\mathbf{r}_1)|\tilde{S_2}|^2(\hat{\mathbf{k}}_{0f},\mathbf{r}_2,\mathbf{r}_1)\sigma_{02}\\ &\times(\mathbf{r}_1;\mathbf{r}_2)\tilde{G}_0^m(\mathbf{r}_2,\mathbf{r}_1)|^2|\tilde{S_1}|^2(\mathbf{r}_1,\mathbf{r}_2)\sigma_{01}(\mathbf{r}_1;\mathbf{r}_2)\\ &\times|\tilde{S_0}(\mathbf{r}_1)|^2|\tilde{\phi}_{12}|^2(\mathbf{r}_1,\mathbf{r}_2).\end{aligned} \tag{26}$$

A. Overlap function

The calculation of the square of the overlap function $|\phi_{12}|^2$ from nuclear structure inputs is briefly presented: two-nucleon amplitudes (TNA) and single-particle wave functions. Starting from the expression from [11],

$$\begin{aligned}&|\phi_{12}(\mathbf{r}_1,\mathbf{r}_2)|^2\\ &= \frac{1}{J_i^2}\sum_{M_iM_f}\left\langle\Psi^{(F)}_{J_iM_i}\middle|\Psi^{(F)}_{J_iM_i}\right\rangle = \sum_{\alpha\alpha'I}\frac{C_\alpha^{J_iJ_fI}C_{\alpha'}^{J_iJ_fI}D_\alpha D_{\alpha'}}{I^2}\\ &\times\sum_{m_1m_2m_1'm_2'}\langle j_1m_1j_2m_2|I\mu\rangle\langle j_1'm_1'j_2'm_2'|I\mu\rangle\\ &\times\left[\left(\phi^{m_1'}_{j_1'}\middle|\phi^{m_1}_{j_1}\right)\left(\phi^{m_2'}_{j_2'}\middle|\phi^{m_2}_{j_2}\right) + \left(\phi^{m_2'}_{j_2'}\middle|\phi^{m_2}_{j_2}\right)\left(\phi^{m_1'}_{j_1'}\middle|\phi^{m_1}_{j_1}\right)\right.\\ &\left.- \left(\phi^{m_1'}_{j_1'}\middle|\phi^{m_2}_{j_2}\right)\left(\phi^{m_2'}_{j_2'}\middle|\phi^{m_1}_{j_1}\right) - \left(\phi^{m_2'}_{j_2'}\middle|\phi^{m_1}_{j_1}\right)\left(\phi^{m_1'}_{j_1'}\middle|\phi^{m_2}_{j_2}\right)\right],\end{aligned} \tag{27}$$

where $\Psi^{(F)}_{J_iM_i}$ is the overlap function $\langle A|A+2\rangle$ with J_i, M_i and J_f, M_f being the total and magnetic angular momenta of $A+2$ and A, respectively. $C_\alpha^{J_iJ_fI}$ corresponds to the TNA, $\alpha = l_1, j_1, l_2, j_2$, the orbital and angular momenta of the two removed protons, m_i the corresponding magnetic angular momentum, $D_\alpha = 1/\sqrt{2(1+\delta_{\alpha\alpha'})}$, $\mathbf{I} = \mathbf{j_1} + \mathbf{j_2}$, and the bracket $(\phi^{m_2'}_{j_2'}|\phi^{m_2}_{j_2})$ corresponds to

$$\begin{aligned}\left(\phi^{m_1'}_{j_1'}\middle|\phi^{m_1}_{j_1}\right) = &\sum_{\lambda_1\lambda_1'\sigma}\langle l_1\lambda_1s\sigma|j_1m_1\rangle\langle l_1'\lambda_1's\sigma|j_1'm_1'\rangle\\ &\times u_{l_1j_1}(r_1)Y_{l_1\lambda_1}(\hat{\mathbf{r}_1})u^*_{l_1'j_1'}(r_1)Y^*_{l_1'\lambda_1'}(\hat{\mathbf{r}_1}),\end{aligned} \tag{28}$$

where u_{lj} is the radial wave function, evaluated at $S_{2p}/2$ [11], $Y_{l\lambda}$ the spherical harmonic with magnetic angular momentum λ, and s and σ are the spin of the proton and its projection. Note that in Eq. (27), the first bracket in each term is evaluated for $\mathbf{r}_1$ while the second bracket is evaluated for $\mathbf{r}_2$.

After some angular momentum algebra, the following expression is obtained:

$$
\begin{aligned}
|\tilde{\phi}_{12}|^2(\mathbf{r_1}, \mathbf{r_2}) = \sum_{\alpha\alpha' I} C_{\alpha}^{J_i J_f I} C_{\alpha'}^{J_i J_f I} D_\alpha D_{\alpha'} \frac{\hat{l}_1 \hat{l}'_1 \hat{l}_2 \hat{l}'_2 \hat{j}_1 \hat{j}_2 \hat{j}'_1 \hat{j}'_2}{16\pi^2} (-)^{-s_1-s_2+j_2+j'_2} \sum_L P^L(\mathbf{r_1}\cdot\mathbf{r_2}) \\
\times \Bigg[\Bigg((-)^{I-2j'_2} \langle l_1 0, l'_1 0 | L 0\rangle \langle l_2 0, l'_2 0 | L 0\rangle \begin{Bmatrix} l_1 & s_1 & j_1 \\ j'_1 & L & l'_1 \end{Bmatrix} \begin{Bmatrix} l_2 & s_2 & j_2 \\ j'_2 & L & l'_2 \end{Bmatrix} \begin{Bmatrix} j_1 & I & j_2 \\ j'_2 & L & j'_1 \end{Bmatrix} \Bigg) \\
\times \left(u_{l_1 j_1}(r_1) u^*_{l'_1 j'_1}(r_1) u_{l_2 j_2}(r_2) u^*_{l'_2 j'_2}(r_2) \right) + u_{l_2 j_2}(r_1) u^*_{l'_2 j'_2}(r_1) u_{l_1 j_1}(r_2) u^*_{l'_1 j'_1}(r_2) \\
- \Bigg(\langle l_1 0, l'_2 0 | L 0\rangle \langle l_2 0, l'_1 0 | L 0\rangle \begin{Bmatrix} l_1 & s_1 & j_1 \\ j'_2 & L & l'_2 \end{Bmatrix} \begin{Bmatrix} l_2 & s_2 & j_2 \\ j'_1 & L & l'_1 \end{Bmatrix} \begin{Bmatrix} j_1 & I & j_2 \\ j'_1 & L & j'_2 \end{Bmatrix} \Bigg) \\
\times \left(u_{l_2 j_2}(r_1) u^*_{l'_1 j'_1}(r_1) u_{l_1 j_1}(r_2) u^*_{l'_2 j'_2}(r_2) \right) + u_{l_1 j_1}(r_1) u^*_{l'_2 j'_2}(r_1) u_{l_2 j_2}(r_2) u^*_{l'_1 j'_1}(r_2) \Bigg],
\end{aligned}
\tag{29}
$$

where the angular dependence on $\hat{\mathbf{r}}_1$ and $\hat{\mathbf{r}}_2$ is reduced to the Legendre polynomial $P^L(\mathbf{r_1}\cdot\mathbf{r_2})$, which allows for more efficient treatment of the overlap wave function, which can be stored as a function of r_1, r_2 (only the modulus) and L, instead of $\mathbf{r}_1$ and $\mathbf{r}_2$.

III. NUMERICAL RESULTS

For all the following calculations the optical potential between proton and nucleus has been taken from the global Dirac parametrization [26,27], while the proton-proton elastic cross section has been taken from the parametrization by Bertulani and De Conti [28]. The single-particle wave functions have been computed using Woods-Saxon potentials with diffusivity $a = 0.7$ fm and a radius adjusted to reproduce the rms radius from Hartree-Fock calculations using the SkX interaction [29]. The integration over r_1 and r_2 is extended up to the radius where the single-particle wave functions is reduced to $1/1000$ of their maximum value (the maximum radius among the wave functions) and the step of integration is taken as 0.2 fm, which was found to give converged results to ≈5%.

A. ^{12}C$(p, 3p)$ ^{10}Be

First, a study of the ^{12}C$(p, 3p)$ ^{10}Be reaction is presented. Admittedly, the ^{12}C nucleus is rather light while the formalism developed in this work is meant for heavier systems. An estimation of the effect of the finite mass of the nucleus can be obtained from [25], which presents a very similar result to the one in this work in the context of the study of the total nucleon-nucleus cross section. In [25], the cross section is scaled by a factor of $(\frac{A}{A+1})^4$, which in this case would introduce a factor of 0.7 in the cross sections. As the ambiguities in the optical potentials introduce significant uncertainties in the total cross section, this factor will not be considered in the following. The nuclear structure of ^{12}C is well known and there exist experimental data for fragmentation of ^{12}C on proton targets to produce ^{10}Be [30], so this reaction is a reasonable one to benchmark the calculations.

The TNA for the calculation have been obtained using the WBT interaction [31] in the shell model code OXBASH [32] (calculations using the interaction by Cohen and Kurath [33] show consistent TNA). Those TNA deemed too small have been excluded from the calculation. In Table I the used TNA are presented. In order to compare with the total experimental cross section in [30], the calculation has been performed at 1.05 GeV/A. Only states under the neutron emission threshold for ^{10}Be have been considered and their energies have been taken as the experimental ones.

The results are presented in Table II. Since the kinematics of the removed protons was not measured in the experiment, another process that could result in ^{10}Be is a $(p, 2p)$ reaction producing an excited ^{11}B* which then decays by emission of a proton and thus competes with the process studied here [30]. In a recent measurement of the ^{12}C$(p, 2p)$ reaction at 398 MeV/nucleon, the cross section for the ^{12}C$(p, 2p)$ ^{11}B process was found to be 18.1(2.0) mb while the cross section for the decay of ^{11}B* into ^{10}Be (distinguished by imposing a coincidence of a forward proton and ^{10}Be) was 0.8(0.3) mb [34]. Assuming the same proportion for the reaction at 1.05 GeV/A, given that the ^{12}C$(p, 2p)$ ^{11}B cross section was of 30.9(3.4)

TABLE I. TNA used for the ^{12}C$(p, 3p)$ ^{10}Be reaction, not including the isospin Clebsch-Gordan factor, obtained using the WBT interaction.

J^π_f	E_x (MeV)	$[1s_{1/2}]^2$	$[1p_{3/2}]^2$	$[1p_{1/2}1p_{3/2}]$	$[1p_{1/2}]^2$	$[1d_{5/2}]^2$	$[1d_{3/2}]^2$	$[2s_{1/2}]^2$	$[2s_{1/2}1d_{5/2}]$	$[2s_{1/2}1d_{3/2}]$
0^+	0.00	–	1.461	–	0.706	−0.064	−0.056	−0.056	–	–
2^+	3.37	–	2.060	−0.854	–	0.038	0.020	–	–	–
2^+	5.96	–	−0.419	1.204	–	0.028	0.016	–	−0.020	−0.010
0^+	6.18	−0.018	−0.165	–	0.145	–	0.016	–	–	–
J^π_f	E_x (MeV)	$[1p_{3/2}1s_{1/2}]$	$[1p_{1/2}1s_{1/2}]$	$[1d_{5/2}1p_{3/2}]$	$[1d_{5/2}1p_{1/2}]$	$[1d_{3/2}1p_{3/2}]$	$[1d_{3/2}1p_{1/2}]$	$[2s_{1/2}1p_{3/2}]$	$[2s_{1/2}1p_{1/2}]$	
1^-	5.96	−0.247	0.135	−0.117	–	0.069	−0.077	0.065	0.051	
2^-	6.26	0.045	–	−0.048	−0.055	0.105	−0.021	–	–	

TABLE II. Cross sections for the ^{12}C$(p, 3p)$ ^{10}Be(J_f^π) reaction at 1.05 GeV/A.

J_f^π	E_x (MeV)	σ (mb)
0^+	0.00	0.86
2^+	3.37	0.68
2^+	5.96	0.27
1^-	5.96	9.2×10^{-3}
0^+	6.18	4.1×10^{-3}
2^-	6.26	5.5×10^{-4}
Total		1.82
Exp. [30]		3.41(0.54)
Exp. [direct $(p, 3p)$]		2.0(0.7)*

*See text.

mb, this would yield a cross section for excitation-evaporation of 1.4(0.6) mb, leaving 2.0(0.7) mb for the direct removal of the two protons studied in this work, which gives reasonable agreement with the result of the calculations, and thus this result can be taken a validation of this work. It should be remarked that in [5,35], for two-proton removal from ^{12}C using a carbon target at the same beam energy, the excitation-evaporation process was not removed and good agreement between theory and experiment was found still, which could indicate differences between proton and carbon targets when populating proton-unbound excited states of ^{11}B.

B. ^{28}Mg$(p, 3p)$ ^{26}Ne

In this section, the ^{28}Mg$(p, 3p)$ ^{26}Ne reaction at 250 MeV/nucleon is explored. Although no experimental data exists for this reaction, the equivalent two-nucleon knockout reaction with beryllium target has been measured [1] and thoroughly studied [4,5,36], making it a good benchmark to compare the $(p, 3p)$ and two-proton knockout reactions when populating different excited states. The structure inputs are the same as those from [4], the TNA are presented in Table III for completeness.

It is of interest whether $(p, 3p)$ and two-proton knockout reactions populate equally the excited states of the residual nucleus, as such in Table IV cross sections are presented for the four considered states for the $(p, 3p)$ reaction at 250 MeV/nucleon, a typical energy for radioactive beam facilities, as well as the two-proton knockout reaction at 82.3 MeV/nucleon [1], and their ratio to the total cross section. Experimental results for the two-proton knockout reaction are presented as well. The theoretical and experimental results for the two-proton knockout reaction are taken from [36] and [4], respectively.

In general, the distribution of the cross section among states is similar for both reactions, with the ground and 4^+ excited states taking most of the cross section, although it should be noted that the contribution of the ground state is significantly larger for the $(p, 3p)$ reaction than for the two-proton knockout one. To further explore this discrepancy a calculation has been performed in which the interference between configurations with different TNA has been turned off in order to evaluate the effect of this interference in the cross section. The results are shown on the third column of Table IV, while the fourth column shows the ratio between these calculations and the original ones. It is noteworthy that it is the ground state that presents the most sensitivity to this interference, suggesting that the interference lies behind the difference between $(p, 3p)$ and knockout, possibly because $(p, 3p)$ is more sensitive to the nuclear interior, which presents a different behavior than the nuclear surface with respect to the interference of different configurations. This suggests that interference between configurations and correlations between the removed protons plays a significant role in two-proton-removal reactions [35,36], and that $(p, 3p)$ and two-proton knockout reactions may be differently sensitive to them. The last two columns of Table IV show the sum of the square of the TNA and their ratio to the total for each ^{26}Ne final state, to check whether a direct relation between the reaction cross section and the structure observables, akin to spectroscopic factors for one-nucleon removal reactions, can be established for two-nucleon removal ones. As expected, this is not the case, as the contribution of each final state to the total cross section differs significantly from its "weight", measured as the sum of the square of the TNAs. Therefore a robust reaction theory is essential to be able to predict the relative population of each final state, although a rough relation can be established between TNA and cross sections, in that states with a small sum of TNA^2 can be expected to be weakly populated and a state with a large sum is likely to be significantly populated.

C. ^{54}Ca$(p, 3p)$ ^{52}Ar

Although there is a number of medium-mass nuclei for which the $(p, 3p)$ reaction has been measured [22], for these nuclei the nuclear structure calculations are computationally heavy and the experimental data scarce, so there are significant uncertainties in the TNA (admittedly, also in the optical potentials). As such, it is challenging to find neutron-rich nuclei to compare their experimental cross sections to the results of this work. For the ^{54}Ca$(p, 3p)$ ^{52}Ar reaction, unpublished

TABLE III. TNA used for the ^{28}Mg$(p, 3p)$ ^{26}Ne reaction, taken from [4].

J_f^π	E_x (MeV)	$[1d_{3/2}]^2$	$[1d_{3/2}1d_{5/2}]$	$[1d_{5/2}]^2$	$[2s_{1/2}1d_{3/2}]$	$[2s_{1/2}1d_{5/2}]$	$[2s_{1/2}]^2$
0^+	0.00	−0.301	–	−1.047	–	–	−0.305
2^+	2.02	−0.050	0.374	−0.637	−0.061	−0.139	–
4^+	3.50	–	0.331	1.596	–	–	–
2^+	3.70	0.047	−0.072	0.853	0.161	0.176	–

TABLE IV. Cross sections for the ^{28}Mg$(p, 3p)^{26}$Ne(J_f^π) reaction at 250 MeV/nucleon (third column) and the ^{9}Be$(^{28}$Mg, ^{26}Ne$(J_f^\pi))X$ reaction at 82.3 MeV/nucleon (seventh column [36], ninth column [4]), and the ratio of each ^{26}Ne final state to the total cross section (second and sixth columns, respectively). The third column corresponds to calculations where configurations with different TNA are not allowed to interfere and the fourth column is the ratio between this calculation and the full one. The tenth column corresponds to the sum of the square of the TNA considered for each state, and the 11th column to its ratio to the total adding all final states.

J_f^π	E_x (MeV)	$\sigma(p, 3p)$ (mb)	Ratio	$\sigma(p, 3p)$ no interf. (mb)	$\frac{(p,3p)^{\text{nointerf.}}}{(p,3p)}$	$\sigma 2p$KO (mb)	Ratio	Exp $2p$KO (mb)	$\sum$TNA^2	Ratio
0^+	0.00	0.274	0.48	0.196	0.71	1.19	0.40	0.70(15)	1.28	0.24
2^+	2.02	0.048	0.08	0.048	1.00	0.32	0.11	0.09(15)	0.69	0.13
4^+	3.50	0.181	0.32	0.160	0.88	1.02	0.34	0.58(9)	2.66	0.49
2^+	3.70	0.063	0.11	0.061	0.97	0.45	0.15	0.15(9)	0.79	0.15
Total		0.57		0.46		2.98		1.50(10)	5.42	

experimental data at 250 MeV/nucleon were facilitated to the author [37], yielding a total cross section of $\sigma = 0.047(6)$ mb. For $\langle^{54}$Ca $|\, ^{52}$Ar$\rangle$, TNA have been provided by Prof. Y. Utsuno [38], obtained using an extension of the GXPF1Br [39] interaction extended to the sd-pf-sdg space. The ones considered in these calculations are presented in Table V. When considering which states to include, a significant strength can be found close to the separation energy of the neutron S_n in ^{52}Ar. Taking the values from NuDat [40], $S_n = 3.0(7)$ MeV, obtained by a systematic fit to the nuclear mass, so there is an ambiguity on whether the population of states with excitation energy $E_x = 3.0$–3.7 MeV would lead to a bound residual ^{52}Ar (thus contributing to the cross section), or not.

To check the effect of this ambiguity the cross section to all states for energies up to 3.7 MeV has been computed, and are presented adding up the states up to $E_x = 3.0$ MeV (which corresponds to the nominal value of S_n) and up to $E_x = 3.7$ MeV (which would also include the states within the 1σ error range). Both values yield results of 0.102 mb and 0.159 mb, which shows that even the uncertainty in S_n produces differences of 50% in the results. Better measurements of the masses of medium-mass nuclei or measurements of $(p, 3p)$ reactions with γ coincidence would help alleviate this ambiguity. As for the reduction factors, values of $R_s = 0.46$ and 0.29 are found, both of which are reasonably compatible to those found in [41,42], even when considering the uncertainties in the separation energy. The reduction factors for two-nucleon knockout [36,41,42] (also including two-neutron knockout from proton-rich nuclei) and $(p, 3p)$ reactions are presented in Fig. 2 as a function of the difference between the separation energy of two protons and two neutrons $\Delta S = S_{2p} - S_{2n}$ for two-proton knockout and $(p, 3p)$ and $S_{2n} - S_{2p}$ for two-neutron knockout, as a parallel to the renowned figure for single-nucleon removal [43–45]. R_s for two-proton(neutron) knockout correspond to the blue circles(squares) while the red diamonds correspond to the $(p, 3p)$ reactions studied in this work. As can be seen in the figure the tendency is similar for both reactions, showing factors $\approx$1 for $\Delta S \approx 0$ and a significant, roughly constant reduction for more asymmetric nuclei. It is quite remarkable that both reactions show similar trends in the description of the cross sections, while for single-nucleon removal reactions a different trend was found for the reduction factors on $\Delta S = S_{n(p)} - S_{p(n)}$ for one-nucleon knockout and $(p, 2p)$ reactions [46], which has been alleged to originate from deficiencies in the reaction mechanism [47] or in the description of the wave functions of the removed nucleons [48–50]. The fact that the trends reconcile for two-nucleon removal reactions

TABLE V. States, TNA, and cross sections considered for the ^{54}Ca$(p, 3p)^{52}$Ar reaction. The last column corresponds to the reduction factor $R_s = \sigma_{\text{exp}}/\sigma_{th}$. States above the double horizontal line lie below the nominal value of S_n for ^{52}Ar, while those below lie below its value plus one σ [40].

J_f^π	E_x (MeV)	$[1d_{5/2}]^2$	$[1d_{5/2}1d_{3/2}]$	$[1d_{5/2}2s_{1/2}]$	$[1d_{3/2}]^2$	$[1d_{3/2}2s_{1/2}]$	$[2s_{1/2}]^2$	σ_{p3p} (mb)	R_s
0^+	0.00	−0.221	–	–	−0.839	–	−0.222	3.51×10^{-2}	
2^+	1.719	−0.205	−0.238	−0.277	−1.187	0.650	–	4.82×10^{-2}	
0^+	2.356	0.053	–	–	0.277	–	−0.030	2.75×10^{-3}	
2^+	2.364	0.118	0.074	0.192	0.575	−0.492	–	1.54×10^{-2}	
3^+	2.809	–	0.029	−0.013	–	–	–	1.35×10^{-5}	
2^+	3.012	0.167	0.077	0.052	1.378	−0.147	–	3.32×10^{-2}	
3^+	3.363	–	−0.077	−0.013	–	–	–	7.62×10^{-5}	
4^+	3.464	0.073	0.318	–	–	–	–	2.57×10^{-3}	
4^+	3.592	0.0511	0.355	–	–	–	–	3.00×10^{-3}	
2^+	3.639	−0.017	0.108	0.263	−0.678	−0.984	–	1.89×10^{-2}	
0^+	3.670	0.001	–	–	0.089	–	−0.096	2.97×10^{-4}	
Total ($E_x^{\max} = S_n = 3.0$ MeV)								1.02×10^{-1}	0.46
Total ($E_x^{\max} = S_n + \sigma_{S_n} = 3.7$ MeV)								1.59×10^{-1}	0.29

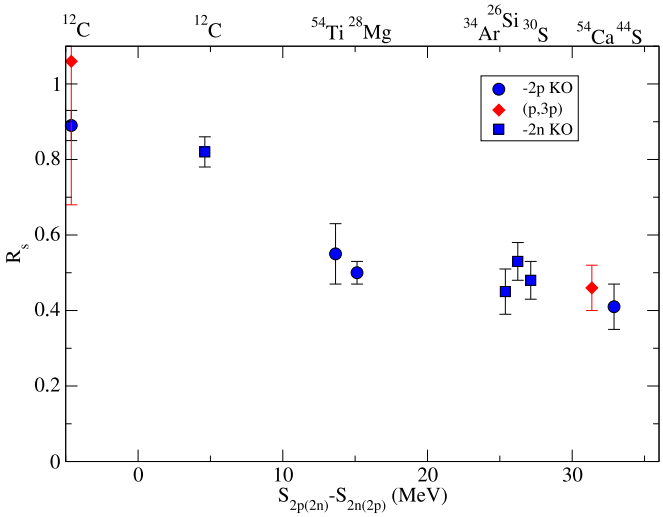

FIG. 2. Reduction factors for two-proton (blue circles) and two-neutron (blue squares) knockout reactions [36,41,42] and $(p, 3p)$ reactions, as a function of $S_{2p} - S_{2n}$ for two-proton removal and $S_{2s} - S_{2p}$ for two-neutron removal. It can be seen that the two types of reactions follow similar trends.

could be related to the stronger peripherality of these reactions [11], when compared to one-nucleon removal ones, so that the nuclear interior, where the reaction mechanism and the wave functions are less understood, plays a smaller role in the reaction. Further study on these trends is required to clarify these issues.

IV. SUMMARY AND CONCLUSIONS

In this work, a theoretical description of the sequential $(p, 3p)$ two-proton removal direct reaction is presented, which is able to produce cross sections for specific states of the final nucleus based on the two-nucleon amplitudes from nuclear structure calculations. This theory relies on the eikonal description of the interaction between protons and nucleus and the assumption of quasifree collisions between the incoming proton and the removed protons. This theory has been validated through comparison with experimental data for the ^{12}C$(p, 3p)$ ^{10}Be reaction, finding reasonable agreement. The ^{28}Mg$(p, 3p)$ ^{26}Ne reaction has also been studied, finding parallels with the results found in two-proton knockout reactions with heavier targets and the theory has been applied to the ^{54}Ca$(p, 3p)$ ^{52}Ar reaction, finding an overestimation of the cross section of a factor ≈2–3, which is consistent with results found in two-proton knockout reactions. This contrasts with the discrepancy found in single-nucleon reactions. Further study on the two-nucleon-removal trends may prove illuminating for the still-unknown causes of the one-nucleon-removal reactions discrepancy. Application of this formalism to other targets, such as those measured in [22] or [21], requires the production of two-nucleon amplitudes, which can prove challenging for these heavy nuclei. Further developments of this work may include the use of microscopic optical potentials for the exotic cases where global parametrizations may prove less reliable, as well as the development of a theory to obtain the momentum distribution of the residual target and the angular correlation between the outgoing protons.

ACKNOWLEDGMENTS

The author thanks Y. Utsuno for providing the two-nucleon amplitudes used for the ^{54}Ca case and H. Liu for the access to the preliminary experimental data for ^{54}Ca. The author would like to thank as well J. Gómez-Camacho, A. M. Moro, and A. Obertelli for illuminating discussions and critical reading of the manuscript. The author acknowledges financial support by MCIN/AEI/10.13039/501100011033 under I+D+i Project No. PID2020-114687GB-I00 and under Grant No. IJC2020-043878-I (also funded by "European Union NextGenerationEU/PRTR"), by the Consejería de Economía, Conocimiento, Empresas y Universidad, Junta de Andalucía (Spain) and "ERDF-A Way of Making Europe" under PAIDI 2020 Project No. P20_01247, by the European Social Fund and Junta de Andalucía (PAIDI 2020) under Grant No. DOC-01006 and by the Alexander von Humboldt Foundation.

[1] D. Bazin, B. A. Brown, C. M. Campbell, J. A. Church, D. C. Dinca, J. Enders, A. Gade, T. Glasmacher, P. G. Hansen, W. F. Mueller, H. Olliver, B. C. Perry, B. M. Sherrill, J. R. Terry, and J. A. Tostevin, Phys. Rev. Lett. **91**, 012501 (2003).

[2] J. Fridmann, I. Wiedenhöver, A. Gade, L. T. Baby, D. Bazin, B. A. Brown, C. M. Campbell, J. M. Cook, P. D. Cottle, E. Diffenderfer, D.-C. Dinca, T. Glasmacher, P. G. Hansen, K. W. Kemper, J. L. Lecouey, W. F. Mueller, H. Olliver, E. Rodriguez-Vieitez, J. R. Terry, J. A. Tostevin, and K. Yoneda, Nature (London) **435**, 922 (2005).

[3] K. Yoneda, A. Obertelli, A. Gade, D. Bazin, B. A. Brown, C. M. Campbell, J. M. Cook, P. D. Cottle, A. D. Davies, D.-C. Dinca, T. Glasmacher, P. G. Hansen, T. Hoagland, K. W. Kemper, J.-L. Lecouey, W. F. Mueller, R. R. Reynolds, B. T. Roeder, J. R. Terry, J. A. Tostevin, and H. Zwahlen, Phys. Rev. C **74**, 021303(R) (2006).

[4] J. A. Tostevin, G. Podolyák, B. A. Brown, and P. G. Hansen, Phys. Rev. C **70**, 064602 (2004).

[5] J. Tostevin, P. Batham, G. Podolyák, and I. Thompson, Nucl. Phys. A **746**, 166 (2004).

[6] J. Fridmann, I. Wiedenhöver, A. Gade, L. T. Baby, D. Bazin, B. A. Brown, C. M. Campbell, J. M. Cook, P. D. Cottle, E. Diffenderfer, D.-C. Dinca, T. Glasmacher, P. G. Hansen, K. W. Kemper, J. L. Lecouey, W. F. Mueller, E. Rodriguez-Vieitez, J. R. Terry, J. A. Tostevin, K. Yoneda, and H. Zwahlen, Phys. Rev. C **74**, 034313 (2006).

[7] A. Gade, R. V. F. Janssens, D. Bazin, R. Broda, B. A. Brown, C. M. Campbell, M. P. Carpenter, J. M. Cook, A. N. Deacon, D.-C. Dinca, B. Fornal, S. J. Freeman, T. Glasmacher, P. G. Hansen, B. P. Kay, P. F. Mantica, W. F. Mueller, J. R. Terry, J. A. Tostevin, and S. Zhu, Phys. Rev. C **74**, 021302(R) (2006).

[8] A. Gade, P. Adrich, D. Bazin, M. D. Bowen, B. A. Brown, C. M. Campbell, J. M. Cook, S. Ettenauer, T. Glasmacher, K. W. Kemper, S. McDaniel, A. Obertelli, T. Otsuka, A. Ratkiewicz, K. Siwek, J. R. Terry, J. A. Tostevin, Y. Utsuno, and D. Weisshaar, Phys. Rev. Lett. **99**, 072502 (2007).

[9] B. Bastin, S. Grévy, D. Sohler, O. Sorlin, Z. Dombrádi, N. L. Achouri, J. C. Angélique, F. Azaiez, D. Baiborodin, R. Borcea, C. Bourgeois, A. Buta, A. Bürger, R. Chapman, J. C. Dalouzy, Z. Dlouhy, A. Drouard, Z. Elekes, S. Franchoo, S. Iacob, B. Laurent, M. Lazar, X. Liang, E. Liénard, J. Mrazek, L. Nalpas, F. Negoita, N. A. Orr, Y. Penionzhkevich, Z. Podolyák, F. Pougheon, P. Roussel-Chomaz, M. G. Saint-Laurent, M. Stanoiu, I. Stefan, F. Nowacki, and A. Poves, Phys. Rev. Lett. **99**, 022503 (2007).

[10] P. Adrich, A. M. Amthor, D. Bazin, M. D. Bowen, B. A. Brown, C. M. Campbell, J. M. Cook, A. Gade, D. Galaviz, T. Glasmacher, S. McDaniel, D. Miller, A. Obertelli, Y. Shimbara, K. P. Siwek, J. A. Tostevin, and D. Weisshaar, Phys. Rev. C **77**, 054306 (2008).

[11] E. C. Simpson, J. A. Tostevin, D. Bazin, and A. Gade, Phys. Rev. C **79**, 064621 (2009).

[12] E. C. Simpson and J. A. Tostevin, Phys. Rev. C **79**, 024616 (2009).

[13] K. Wimmer, D. Bazin, A. Gade, J. A. Tostevin, T. Baugher, Z. Chajecki, D. Coupland, M. A. Famiano, T. K. Ghosh, G. F. Grinyer, R. Hodges, M. E. Howard, M. Kilburn, W. G. Lynch, B. Manning, K. Meierbachtol, P. Quarterman, A. Ratkiewicz, A. Sanetullaev, E. C. Simpson, S. R. Stroberg, M. B. Tsang, D. Weisshaar, J. Winkelbauer, R. Winkler, and M. Youngs, Phys. Rev. Lett. **109**, 202505 (2012).

[14] S. Beceiro-Novo, T. Ahn, D. Bazin, and W. Mittig, Prog. Part. Nucl. Phys. **84**, 124 (2015).

[15] A. Obertelli, A. Delbart, S. Anvar, L. Audirac, G. Authelet, H. Baba, B. Bruyneel, D. Calvet, F. Château, A. Corsi, P. Doornenbal, J.-M. Gheller, A. Giganon, C. Lahonde-Hamdoun, D. Leboeuf, D. Loiseau, A. Mohamed, J. P. Mols, H. Otsu, C. Péron, A. Peyaud, E. C. Pollacco, G. Prono, J.-Y. Rousse, C. Santamaria, and T. Uesaka, Eur. Phys. J. A **50**, 8 (2014).

[16] P. Hansen and J. Tostevin, Annu. Rev. Nucl. Part. Sci. **53**, 219 (2003).

[17] G. Jacob and T. A. J. Maris, Rev. Mod. Phys. **38**, 121 (1966).

[18] T. Aumann, C. A. Bertulani, and J. Ryckebusch, Phys. Rev. C **88**, 064610 (2013).

[19] A. M. Moro, Phys. Rev. C **92**, 044605 (2015).

[20] K. Ogata, K. Yoshida, and K. Minomo, Phys. Rev. C **92**, 034616 (2015).

[21] R. Taniuchi, C. Santamaria, P. Doornenbal, A. Obertelli, K. Yoneda, G. Authelet, H. Baba, D. Calvet, F. Château, A. Corsi, A. Delbart, J.-M. Gheller, A. Gillibert, J. D. Holt, T. Isobe, V. Lapoux, M. Matsushita, J. Menéndez, S. Momiyama, T. Motobayashi, M. Niikura, F. Nowacki, K. Ogata, H. Otsu, T. Otsuka, C. Péron, S. Péru, A. Peyaud, E. C. Pollacco, A. Poves, J.-Y. Roussé, H. Sakurai, A. Schwenk, Y. Shiga, J. Simonis, S. R. Stroberg, S. Takeuchi, Y. Tsunoda, T. Uesaka, H. Wang, F. Browne, L. X. Chung, Z. Dombradi, S. Franchoo, F. Giacoppo, A. Gottardo, K. Hadyńska-Klęk, Z. Korkulu, S. Koyama, Y. Kubota, J. Lee, M. Lettmann, C. Louchart, R. Lozeva, K. Matsui, T. Miyazaki, S. Nishimura, L. Olivier, S. Ota, Z. Patel, E. Şahin, C. Shand, P.-A. Söderström, I. Stefan, D. Steppenbeck, T. Sumikama, D. Suzuki, Z. Vajta, V. Werner, J. Wu, and Z. Y. Xu, Nature (London) **569**, 53 (2019).

[22] A. Frotscher, M. Gómez-Ramos, A. Obertelli, P. Doornenbal, G. Authelet, H. Baba, D. Calvet, F. Château, S. Chen, A. Corsi, A. Delbart, J.-M. Gheller, A. Giganon, A. Gillibert, T. Isobe, V. Lapoux, M. Matsushita, S. Momiyama, T. Motobayashi, M. Niikura, H. Otsu, N. Paul, C. Péron, A. Peyaud, E. C. Pollacco, J.-Y. Roussé, H. Sakurai, C. Santamaria, M. Sasano, Y. Shiga, N. Shimizu, D. Steppenbeck, S. Takeuchi, R. Taniuchi, T. Uesaka, H. Wang, K. Yoneda, T. Ando, T. Arici, A. Blazhev, F. Browne, A. M. Bruce, R. Carroll, L. X. Chung, M. L. Cortés, M. Dewald, B. Ding, Z. Dombradi, F. Flavigny, S. Franchoo, F. Giacoppo, M. Górska, A. Gottardo, K. Hadyńska-Klęk, Z. Korkulu, S. Koyama, Y. Kubota, A. Jungclaus, J. Lee, M. Lettmann, B. D. Linh, J. Liu, Z. Liu, C. Lizarazo, C. Louchart, R. Lozeva, K. Matsui, T. Miyazaki, K. Moschner, S. Nagamine, N. Nakatsuka, C. Nita, S. Nishimura, C. R. Nobs, L. Olivier, S. Ota, Z. Patel, Z. Podolyák, M. Rudigier, E. Sahin, T. Y. Saito, C. Shand, P.-A. Söderström, I. G. Stefan, T. Sumikama, D. Suzuki, R. Orlandi, V. Vaquero, Z. Vajta, V. Werner, K. Wimmer, J. Wu, and Z. Xu, Phys. Rev. Lett. **125**, 012501 (2020).

[23] M. L. Goldberger and K. M. Watson, *Collision Theory* (John Wiley & Sons, Inc., New York, 1967).

[24] C. J. Joachaim, *Quantum Collision Theory* (North Holland Publishing Company, Amsterdam, 1975).

[25] M. Kawai and H. A. Weidenmüller, Phys. Rev. C **45**, 1856 (1992).

[26] S. Hama, B. C. Clark, E. D. Cooper, H. S. Sherif, and R. L. Mercer, Phys. Rev. C **41**, 2737 (1990).

[27] E. D. Cooper, S. Hama, B. C. Clark, and R. L. Mercer, Phys. Rev. C **47**, 297 (1993).

[28] C. A. Bertulani and C. De Conti, Phys. Rev. C **81**, 064603 (2010).

[29] B. A. Brown, Phys. Rev. C **58**, 220 (1998).

[30] D. L. Olson, B. L. Berman, D. E. Greiner, H. H. Heckman, P. J. Lindstrom, and H. J. Crawford, Phys. Rev. C **28**, 1602 (1983).

[31] E. K. Warburton and B. A. Brown, Phys. Rev. C **46**, 923 (1992).

[32] A. Etchegoyen, W. D. Rae, N. S. Godwin, W. A. Richter, C. H. Zimmerman, B. A. Brown, W. E. Ormand, and J. S. Winfield, MSU-NSCL Report (1985).

[33] S. Cohen and D. Kurath, Nucl. Phys. **73**, 1 (1965).

[34] V. Panin, Ph.D. thesis, Technische Universität Darmstadt, 2012.

[35] E. C. Simpson and J. A. Tostevin, Phys. Rev. C **83**, 014605 (2011).

[36] E. C. Simpson and J. A. Tostevin, Phys. Rev. C **82**, 044616 (2010).

[37] H. Liu (private communication).

[38] Y. Utsuno (private communication).

[39] D. Steppenbeck, S. Takeuchi, N. Aoi, P. Doornenbal, M. Matsushita, H. Wang, H. Baba, N. Fukuda, S. Go, M. Honma, J. Lee, K. Matsui, S. Michimasa, T. Motobayashi, D. Nishimura, T. Otsuka, H. Sakurai, Y. Shiga, P.-A. Söderström, T. Sumikama, H. Suzuki, R. Taniuchi, Y. Utsuno, J. J. Valiente-Dobón, and K. Yoneda, Nature (London) **502**, 207 (2013).

[40] National Nuclear Data Center, information extracted from the NUDAT database, https://www.nndc.bnl.gov/nudat/.

[41] J. A. Tostevin and B. A. Brown, Phys. Rev. C **74**, 064604 (2006).

[42] J. A. Tostevin, B. A. Brown, and E. C. Simpson, Phys. Rev. C **87**, 027601 (2013).

[43] A. Gade, P. Adrich, D. Bazin, M. D. Bowen, B. A. Brown, C. M. Campbell, J. M. Cook, T. Glasmacher, P. G. Hansen, K.

Hosier, S. McDaniel, D. McGlinchery, A. Obertelli, K. Siwek, L. A. Riley, J. A. Tostevin, and D. Weisshaar, Phys. Rev. C **77**, 044306 (2008).
[44] J. A. Tostevin and A. Gade, Phys. Rev. C **90**, 057602 (2014).
[45] J. A. Tostevin and A. Gade, Phys. Rev. C **103**, 054610 (2021).
[46] T. Aumann, C. Barbieri, D. Bazin, C. Bertulani, A. Bonaccorso, W. Dickhoff, A. Gade, M. Gómez-Ramos, B. Kay, A. Moro, T. Nakamura, A. Obertelli, K. Ogata, S. Paschalis, and T. Uesaka, Prog. Part. Nucl. Phys. **118**, 103847 (2021).
[47] M. Gómez-Ramos, J. Gómez-Camacho, and A. Moro, Phys. Lett. B **847**, 138284 (2023).
[48] C. A. Bertulani, A. Idini, and C. Barbieri, Phys. Rev. C **104**, L061602 (2021).
[49] J. Li, C. A. Bertulani, and F. Xu, Phys. Rev. C **105**, 024613 (2022).
[50] C. Bertulani, Phys. Lett. B **846**, 138250 (2023).